Hydrocracking of Waste Cooking Oil as Renewable Fuel on NiW/SiO_2-Al_2O_3 Catalyst

S.A. Hanafi, M.S. Elmelawy, H.A. El-Syed and Nasser H. Shalaby*

Egyptian Petroleum Research Institute, Nasr City 11727, Cairo, Egypt

Abstract: Considering the plant-derived oil as a renewable source for production of alternative fuel, the waste cooking oil (WCO) was directly converted in this work as an alternative fuel by using the commercially available NiW/SiO_2-Al_2O_3 hydrocracking catalyst. This conversion was performed in a fixed bed flow reactor at varying operating conditions of temperature (375-450°C), pressure (2, 6 MPa), and LHSV (1, 2, $4h^{-1}$). The H_2/WCO ratio was kept constant at 400 V/V. The distribution of fuel fractions was evaluated via ASTM distillation. The GC was used for analysis of individual hydrocarbon products. The FTIR was used to investigate the progress of oil conversion. The results showed that the catalytic hydrocracking of WCO generates fuels that have chemical and physical properties comparable to those specified for petroleum-based fuels. The amount of kerosene/diesel fractional product decreased with increasing the temperature and pressure and decreasing the LHSV; while gasoline fuel increased. The reaction was found to follow the second order mechanism, where the estimated activation energy E_a was 56 kj mol^{-1}.

Keywords: Hydrocracking, Waste cooking oil, Renewable fuel production.

1. INTRODUCTION

Renewable transportation fuels are generally defined as those fuels derived from the processing and upgrading of various biomass and degradable municipal waste feedstocks. Typical products are hydrogen, methane, propane, ethanol, butanol, gasoline and diesel. Renewable fuels are often classified into three generations, those produced from: (i) conventional processing of edible feedstocks, *e.g.*, can (ethanol via fermentation, biodiesel via esterification); (ii) advanced processing of non-edible feedstocks such as waste greases and lignocelluloses by gasification, hydroprocessing and pyrolysis and (iii) harvesting and advanced processing of ultra-high yield biomass (*e.g.*, algae). The biomass itself may be broken down into three basic categories, carbohydrates, lignin and fats/oils. Carbohydrates primarily include cellulose and hemicellulose fractions. Fats are mainly comprised of triglycerides and fatty acids [1, 2]. The various bio-refining strategies for upgrading these fractions into chemicals and fuels have adequately been outlined [3-6].

The development of alternative fuels from plant-derived oils (such as sunflower, palm, rapeseed, algal oil and their derivatives) as a substitute for fossil fuels has attracted more attention due to the increased demand of environmental concerns and depletion of fossil fuel resources [7, 8]. The demand for green diesel is now increasing, as projected to reach 900 million tons by 2020 [9]. The common ways to produce diesel-type fuel from biomass are: a) by transesterification of triglycerides to obtain biodiesel, being a mixture of fatty acid methyl esters (FAME) and b) by hydro-processing to synthesize green diesel, which is a mixture of hydrocarbons, mainly heptadecane and octadecane. Both fuels can be used as additives to petro-diesel.

The reactions that occur in hydroprocessing can be classified into two groups: hydrocracking and hydrotreating. Hydrocracking involves destructive hydrogenation, involving conversion of higher molecular weight components in a feedstock to lighter products. Isomerization and cracking of C-C bonds in bigger molecules occur at some extent to produce hydrocarbons within the boiling range of gasoline and diesel. Such treatment requires high temperature and use of high hydrogen pressures to minimize the condensation-chain polymerization reactions, leading to coke formation [10]. From catalytic point of view, hydrocracking is carried out on acid supports, *e.g.*, amorphous supports (alumino-silicates), crystalline supports (zeolites) and silico-alumino-phosphates (SAPO) [11]. Hydrotreating involves non-destructive hydrogenation. Mild temperature and hydrogen pressures are employed, so that only the more unstable compounds that might lead to the formation of gums or insoluble materials are converted to more stable compounds [10]. Hydrotreating takes place usually on the metal active sites of a catalyst, *e.g.*, NiMo or CoMo supported on γ-Al_2O_3 [11, 12]. Supported noble metal catalysts are also used [13]. During hydro-processing of triglycerides, the type of catalyst is one of the most important factors to

*Address correspondence to this author at the Egyptian Petroleum Research Institute, Nasr City 11727, Cairo, Egypt; Tel: +20 222745902;
Fax: +20 222747433; E-mail: chem.shalaby@gmail.com

E-ISSN: 2408-9834/15

determine the yield and composition of liquid fuel products, such as green naphtha (C_5-C_9), greenjet fuel (C_{10}-C_{13}) and green diesel (C_{14}-C_{20}). Moreover, the product distribution, the yield and selectivity of hydrocarbons as well as the conversion of plant-derived oil were affected not only by the catalysts but also by the operating conditions. Bezergianni *et al*. [14, 15] investigated the process parameters like temperature, LHSV, pressure and H_2/oil ratio in the hydrotreating of waste cooking oil and found that the temperature, LHSV, pressure and H_2/oil ratio have significant influences on the catalyst performance.

Although the reaction pathway has not been fully understood up till now, there is a consensus that the reaction occurs via the three pathways: hydrodeoxygenation (HDO), decarbonylation (DCO) or decarboxylation (DCO_2) [16-18]. In addition, long chain fatty acids can also abandon oxygen by direct cracking into shorter acids and alkanes, including oxygenate intermediates [12]. Toba *et al*. [19] studied the HDO of waste cooking oil (WCO**)** over sulfided NiMo/Al_2O_3, CoMo/Al_2O_3 and NiW/ Al_2O_3 catalysts. Alumina-supported NiW and NiMo showed higher activity for HDO than CoMo/ alumina, which is susceptible to deactivation. The NiW/Al_2O_3 catalyst led mainly to DCO_2, in contrast to the NiMo and CoMo catalysts. Tiwari *et al*. [20] used meso- porous SiO_2-Al_2O_3 as supports for sulfided NiMo and NiW in the hydroprocessing of waste soya oil mixture with refinery oil. The NiW/ SiO_2-Al_2O_3 catalyst favored hydrocracking for selective production of paraffin-range hydrocarbons via decarboxy-lation and decarbonylation. NiW catalyst showed also good oxygen removal activity. As only few works have been devoted to systematic investigation of the hydrocracking process of plant-derived oil using sulfided NiW/ SiO_2-Al_2O_3 catalyst, the present work was undertaken to follow up the effect of process parameters, viz., temperature, pressure and LHSV, on the hydrocracking of waste cooking oil (WCO), including the distribution of individual hydrocarbons component. A kinetic study was also presented.

2. EXPERIMENTAL

2.1. Materials

Waste cooking oil (WCO) feedstock was obtained from local fast-food restaurants. The WCO was filtered through filter paper to remove solid impurities and was heated with stirring for 3h at 110° C to remove moisture prior to analysis and treatment.

The used DHC-8, as an amorphous hydrocracking catalyst consisting of non-noble hydrogenation metals on a silica-alumina base, was provided by UOP.

2.2. Characterization

2.2.1. Physicochemical Properties of Waste Cooking Oil and Catalyst Used

The elemental composition of WCO was determined using an elemental analyzer with channel control model (Pw 1390-Philips) and spectrometer model Pw 1410 (Table **1**). The chemical composition of WCO was analyzed using an Agilent 6890N FID-GC with an Omnistar Q-mass. A HP-624 capillary column was used to separate the free fatty acids (Table **1**). Physical characterization of WCO is given in Table **2**.

For the used catalyst (supplied by UOP), the BET surface area and pore volume were determined through N_2 adsorption-desorption at -196° C, using Micrometrics Gimini 2375 surface area analyzer. The

Table 1: Composition of WCO Feedstock

Elemental Composition, wt.% (ASTM D4294-90)	**Carbon 77.58**	**Hydrogen 11.63**	**Nitrogen 0.04**	**Sulfur Nil**	**Oxgen 10.36**
Species of fatty acids in WCO feedstock	Formula	Name	Structure	Content g/100g-FFA	
	$C_{16}H_{32}O_2$	Palmitic	C16:0	6.3	
	$C_{16}H_{30}O_2$	Palmitoleic	C16:1	0.2	
	$C_{18}H_{36}O_2$	Stearic	C18:0	5.4	
	$C_{18}H_{34}O_2$	Oleic	C18:1	20	
	$C_{18}H_{32}O_2$	Linoleic	C18:2	68	
	$C_{20}H_{40}O_2$	Aracidic	C20:0	0.1	
		Others	--	0.1	

Table 2: Physical Characterization of WCO Feedstock

Properties	Value		Standard Methods
Physical characterization			
Density (20°C), g/ml	0.9226		ASTM D4052
Refractive index (70°C)	1.45300		ASTM D1218-92
Pour point, °C	-6		ASTM D97-88
Acid value (mg KOH/g-oil)	5.0		ASTM D664
Average molecular weight, g/mol	856		
Flash point, °C	235		ASTM D93
Viscosity (40°C), mm^2/s	39		ASTM D445
Iodine value	76		ASTM D5554-95
Distillation (vol. %, °C)	IBP	400.0	ASTM D2887
	5%	542.9	
	10%	584.4	
	20%	600.5	
	30%	603.7	
	40%	607.1	
	50%	608.8	
	60%	610.1	
	70%	611.0	
	80%	611.8	
	90%	613.3	
	95%	622.2	

pore volume was determined by pore sizer 9320-V_2-08. The measurement was performed on the sample heated at 200° C for 2h in pure nitrogen. Other main properties of the catalyst are shown in Table **3**.

Before the reaction, the used catalyst was pre-sulphided with spiked cyclohexane using dimethyl disulphide (DMDS, 2 wt %). The spiked cyclohexane was passed through the catalyst bed with a flow rate of 150 ml/min under 3.0 MPa hydrogen pressure and a reaction temperature 260° C for 3h and then 360° C for another 3h.

2.2.2. Hydrocracking Activity Tests

The experiments were carried out in a high-pressure reactor system included in a hydrotreating plant. All the major process parameters were kept with such precision limits as used in the industry. Constant feed rate and H_2/WCO ratio were maintained via a liquid feed pump and a gas flow controller, respectively. The reactor system consisted of a down-flow fixed bed tubular reactor (L=50cm, ID=19mm) of 100 cm^3 effective volume, working without back mixing in three independent heating zones. The reaction products passed through a separation system consisted of cooling unit and a high pressure-low temperature separator.

The product mixtures obtained from WCO hydro cracking were separated into gas phase, water and liquid organic phase. The liquid mixtures collected from the separator contained water, hydrocarbons and

Table 3: Physicochemical Properties of DHC-8 Catalyst

Texture properties		Physical properties				Chemical composition, wt. %		
BET surface area, m^2/g	Pore volume, cc/g	Size, mm	Shape	Bulk density compacted, Kg/m^3		Alumino-Silicates	WO_3	NiO
				Dense	Sock, v			
239	0.36	1.6	Sphere	743.3	704.8	85-95	5-15	2

oxygen containing compounds. After water separation, light (C_5-C_9) hydrocarbons (namely, gasoline) were obtained from the organic fraction by distillation up to 180° C. The residue of atmospheric distillation was separated by vacuum distillation into the target product (viz., kerosene/gas oil boiling range fraction, mainly (C_9-C_{18}) and the residue (> C_{18})).

The applied process parameters were varied as follows: the reaction temperature; 375-450° C, the operating pressure; 2 & 6 MPa, liquid hourly space velocity (LHSV); 1-4h^{-1}, while the H_2/WCO ratio was maintained at 400 V/V. The gaseous products were analyzed using a Varian CP-3800 GC with two detectors: thermal conductivity detector (TCD) for analysis of non-organic gases, using a 7 ft Hysep Q molecular sieve-packed stainless steel column and a flame ionization detector (FID) for C_1-C_5 hydrocarbon separation in a 60 meter capillary column packed with DB-1 silicon oil fused silica by helium at 50º C and 5 min hold. The injector and detector temperatures were 150 and 250º C, respectively. The liquid products were analyzed using Agilent 7890A with FID and 30 meter capillary Hp-5. The column temperatures were programmed as: 50º C for 10 min, rise to 300º C at the rate of 4 ºC/min and nitrogen carrier gas flow of 1.0 ml/min.

The chemical composition of OLPs FTIR was investigated by adopting the ATI Mattson Infinity series apparatus Model 960 M0009. In all tests, the liquid products were analyzed using the ASTM standard methods.

The catalytic activity was expressed in terms of conversion %, *i.e.*, the percentage of heavy fraction of the feed being converted to lighter products during the reaction as

$$Conversion\ (\%) = \frac{\boldsymbol{Feed}\ (400^+) - \boldsymbol{Product}\ (400^+)}{\boldsymbol{Feed}\ (400^+)}\ X\ 100$$

where, $feed_{(400^+)}$ and $product_{(400^+)}$ are the weight percent of the feed and product respectively, which have a boiling point higher than 400°C [21].

The products yields were calculated using the following equation [21]:

$$Yield\ (\%) = \frac{\boldsymbol{Desired\ Product}}{\boldsymbol{Feed}\ (400^+)}\ X\ 100$$

3. RESULTS AND DISCUSSION

3.1. Composition and Property of WCO

Table **1** shows the composition and properties of WCO feedstock. Oxygen content was estimated by difference, nitrogen content was so small (not exceeding 0.04 wt %) and sulfur could not be detected in the WCO. Therefore, the fuels produced from WCO feedstock are regarded as environmentally benign green fuels. As for the physical properties, the acid value of the WCO was 5 mg-KOH/g-oil, indicating that it contained free fatty acids. The iodine value of the oil was 76 g-I_2/100g-oil, indicating that the oil contained many C=C unsaturated bonds. The viscosity at 40°C was 39 mm^2/ s and the density at 20°C was 0.9226 g/ml.

3.2. FTIR Analysis

The chemical composition of renewable fuel products, in comparison with the virgin oil, was investigated using FT-IR (Figure **1**). The spectrum of the virgin waste oil appears to consist prevalently of aliphatic hydrocarbons as evidenced by the appearance of the intense C-H stretching bands of alkanes in the 3008-2850 cm^{-1} region and aliphatic C-H bending of methyl and methylene groups at 1371 cm^{-1} and 1459 cm^{-1}, respectively. The absorption peak observed at 722 cm^{-1} suggests the out of plane bending of alkene. Since vegetable oil is mainly triglyceride, the intense stretching band of the ester appears at 1744 cm^{-1} and those of antisymmetric bridge stretching vibrations of C-O are observed at 1170 cm^{-1} and 1163 cm^{-1} [22]. The FTIR spectrum shows also two weaCabsorption at 2676 and 3416 cm^{-1} for OH of carboxylic acid and H-bonded of alcohol, respectively. In the FTIR spectra of conventional diesel, triglyceride and its hydroprocessing products clearly show the similar absorption bands in the region 3000-2850 cm^{-1} and 1480-1350 cm^{-1} due to C-H stretching vibration, referring to the identical functional groups of alkane in their molecular structures [23, 24]. It is clear that the intensity of the bands at 1744 cm^{-1}, 1170 cm^{-1} and at 1163 cm^{-1} are significantly reduced in the spectra of the cracking products, compared to those of the virgin oil, depending on the operating conditions. These findings seem to be ascribed to the occurrence of deoxygenation reaction. In addition, the pronounced diminution of the intensity of the alkene band (C=C) around 725 cm^{-1} confirms the saturation of the double bonds.

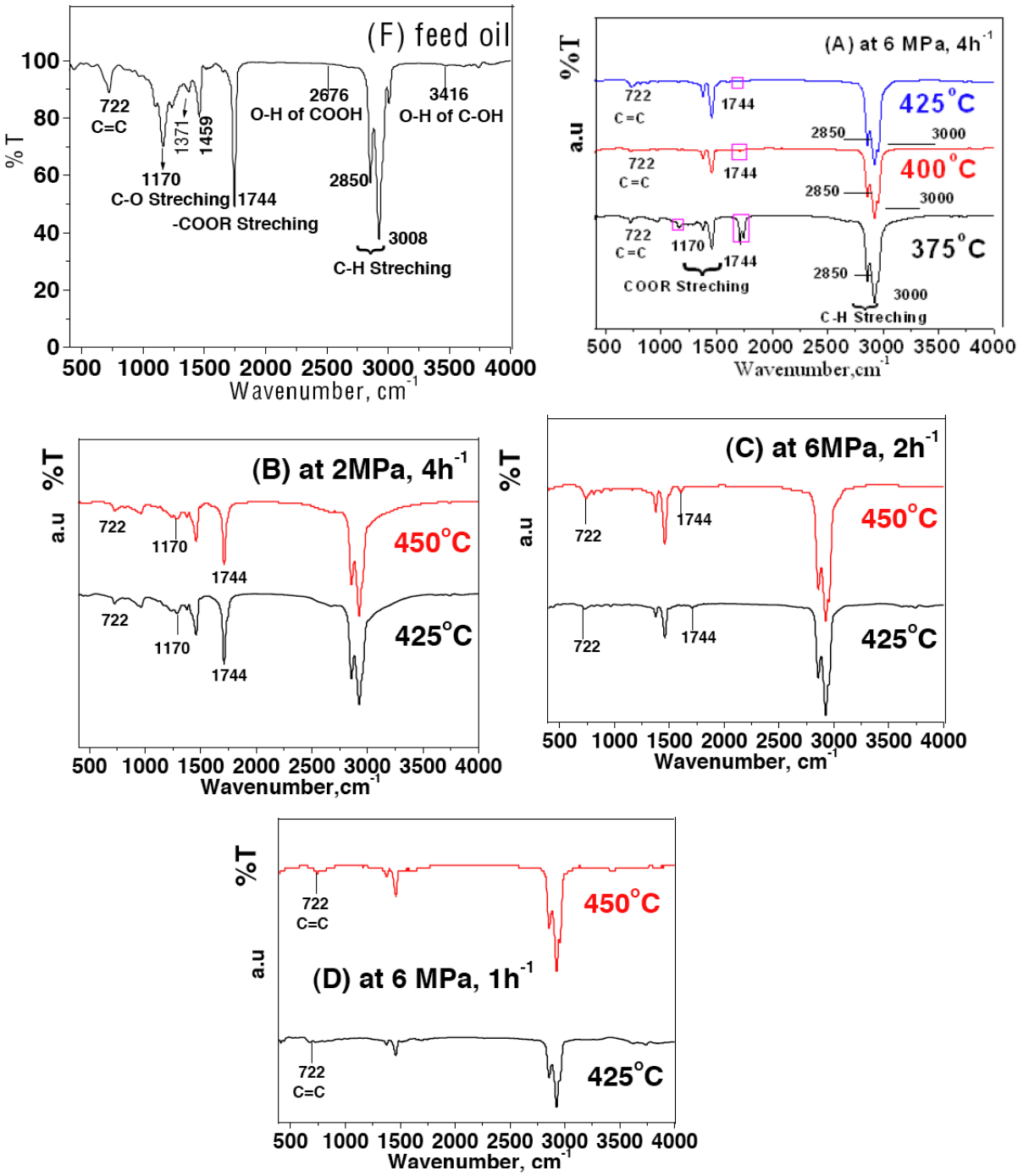

Figure 1: FT-IR spectra of (F) feed oil and cracked products as a function of different reaction parameters.

3.3. Catalytic Conversion

3.3.1. Variation of Temperature

The effect of temperature on the performance of $NiW/SiO_2Al_2O_3$ catalyst was examined in terms of % conversion, yield % of oil liquid product (OLP), gaseous and aqueous phase. Table **4** shows that the conversion of WCO increases steadily with the increase in the reaction temperature due to the higher rate of cracking. The highest conversion was 98.8 wt. % at 450°C, 6.0 MPa and $1h^{-1}$, which may fit with the IR spectra (see Figure**.1**). Similar trends were reported previously confirming the same results [22-24]. The OLP yield % decreases significantly with the increase in temperature at a fixed LHSV and operating pressure. This indicates that a major fraction of OLP (gasoline and middle

Table 4: Effect of Reaction Temperature on Hydrocracking of WCO Feedstock as a Function of LHSVs (Pressure=6MPa, H_2/Oil Ratio = 4 00 v /v)

LHSV, h^{-1}		4				2				1			
Reaction Temperature, °C		375	400	425	450	375	400	425	450	375	400	425	450
Conversion, wt. %		91	94	95.3	96.6	94.7	96.5	97.3	98.1	96.8	98.1	98.4	98.8
Residual oil , wt%, 400^+ °C		9.0	6.0	4.7	3.4	5.3	3.5	2.7	1.9	3.2	1.9	1.6	1.2
Product Distribution Yield, wt.%	Gaseous	13.8	16.5	21.0	23.0	16.3	19.8	22.2	24.4	19.5	21.5	24.0	26.0
	OLP	73.5	71.4	66.3	64.3	71.17	67.0	67.3	61.6	68.0	65.1	60.9	57.5
	Aqueous phase	3.7	6.1	8.0	9.3	7.3	9.7	10.5	12.0	9.3	11.5	13.5	15.3
Gaseous Composition, wt.%	Methane	0.76	1.12	2.07	2.85	--	1.41	2.34	4.0	--	2.5	3.52	5.9
	Ethan and ethylene	2.6	3.69	5.58	8.1	--	5.22	6.03	7.1	--	5.88	9.66	11.39
	Propane and propylene	7.47	6.74	6.58	5.8	--	10.7	10.31	9.0	--	11.59	9.54	7.10
	C_4	3.21	4.32	5.81	5.15	-	1.32	2.03	3.0	-	1.41	1.28	1.61
	C_5	0.46	0.62	0.96	1.1	-	1.15	1.49	1.3	-	0.12	-	-
OLP composition wt. %	Naphtha 45/180°C	26.5	33.0	33.6	34.3	29.5	33.84	35.67	36.93	31.2	35.0	36.4	37.2
	Kerosene /diesel 180/400°C	47.0	38.4	32.7	30.0	41.6	33.14	28.94	24.67	36.8	30.1	24.5	20.3

distillate) has suffered a secondary cracking, resulting in formation of gaseous product. Methane, ethylene, ethane, propylene, propane, and butane were major compounds of the gaseous products (Table **4**). In all possible pathways of the hydrocracking of triglycerides, propane is mainly obtained (Scheme **1**), representing the largest wt % in the gaseous products [25]. It should recalled here, that either CO or CO_2 could not necessarily be observed (if they are formed), as the catalyst could be active enough for the water-gas shift (WGS) equilibrium and methanation of CO and CO_2 in presence of hydrogen and water vapor [25, 26]. It is evident that, the loss of OLP yield had an impact on the yield of the desired products, like gasoline and middle distillate (kerosene and diesel fraction). Generally, the gasoline fraction yield increases with the increase of reaction temperature (Table **4**).

The conversion mechanism represented in Scheme **2** proceeds through several steps. The double bonds and the triglyceride are hydrogenated by one of at least two distinct reaction pathways. The first pathway involves complete hydrogenation, probably via hydrodeoxygenation (HDO) (Reaction 1). The other pathway involves a decarbonylation step, which means that CO is split off (Reaction 2) [22, 23, 27]. As shown in Scheme **2** for a fatty acid with an even carbon number, HDO produces normal paraffins with an even carbon number plus water. The decarbonylation produces normal paraffin with an odd carbon number, water and CO. The decarboxylation (Reaction 3) produces paraffin with an odd carbon number and CO_2.

Both the carbon dioxide and water byproducts are consumed in two additional reactions**:** the reverse water gas shift reaction (Equation 4) and methanation

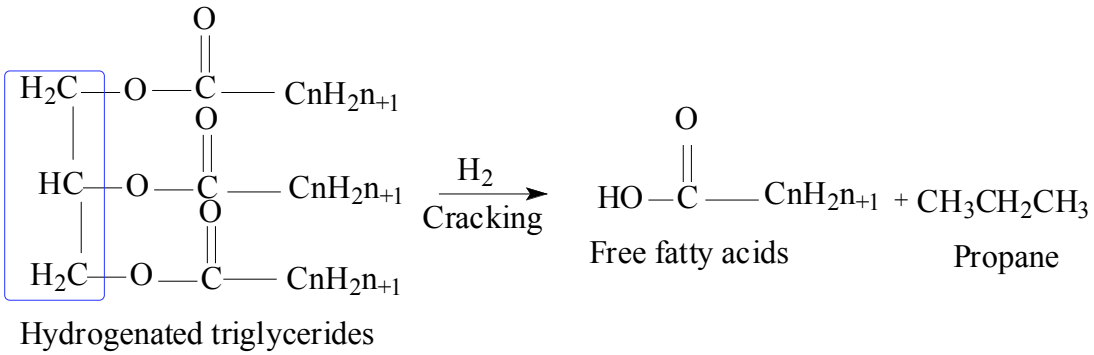

Scheme 1: Cracking of hydrogenated triglycerides.

$C_{17}H_{35}COOH+2H_2$ →	$C_{18}H_{38} + 2H_2O$	Hydrodeoxygenation	(1)
$C_{17}H_{35}COOH +H_2$ →	$C_{17}H_{36}+ 2H_2O + CO$	Decarbonylation	(2)
$C_{17}H_{35}COOH$ →	$C_{17}H_{36} + CO_2$	Decarboxylation	(3)
$CO_2 +H_2$ →	$CO + H_2O$		(4)
$CO + 3H_2$ →	$CH_4 + H_2O$		(5)

Scheme 2: Possible reaction pathways for the hydroprocessing of triglyceride.

reaction (Equation 5). The relative extent of these two reactions accounts for the observed distribution between CO, CO_2, and CH_4.

Table **5** shows the liquid hydrocarbons (OLPs) formed from the hydrocracking of WCO over NiW/SiO_2-Al_2O_3 catalyst. According to Scheme 2, $nC_{18}H_{38}$ and $nC_{16}H_{34}$ are formed by the reduction of the stearic and palmitic acids, respectively, whereas $nC_{15}H_{32}$ and $nC_{17}H_{36}$ are formed by the decarbonylation and decarboxylation of the palmitic acid and stearic acids, respectively. Furthermore, the scission of fatty acid carbon chain is likely following the catalytic cracking carbonium theory [28]. The α-C and β-C are the most active positions, which would generate C_{16} and C_{15} paraffins, as was confirmed by the GC analysis. As the concentration of C_{16} acids in the feedstock is 6.5 wt % (Table **1**) and the change of C_{15} and C_{16} is quite different from C_{17} and C_{18}, it can thus be inferred that the C_{16} and C_{15} hydrocarbons almost come from the α/β – C scission reactions (Scheme **3**). The C_{18}/C_{17} and C_{18}/C_{15}-C_{16} ratios decrease with the increase of temperature (Table **5**). This may indicate that the sensitivity of the different reactions to temperature is as follows: HDO>DCO/DCO_2> α/β – C scission reactions. It can, therefore, be concluded that the high temperature is prone to carry out the catalytic cracking reactions involving the cleavage of the C-C bond, rather than the C-O bond. Similar results were previously reported by Sankaranarayamen [29]. The kerosene/diesel yields (of C_{10}-C_{18} hydrocarbons) dramatically decrease with the increase of temperature (Table **4** and **5**), probably due to the successive cracking reaction of the long chain paraffins, while the product distribution of OLP varies greatly. However, the gasoline yield (of ≤C_9) increases with temperature.

3.2.2. Effect of LHSV

The LHSV is an important operating parameter for controlling the catalyst functionality and the catalyst life, as it determines the time of the feed within the catalyst. To determine the effect of feed space velocity on the hydrocracking process and product yields, three different LHSV values, namely, 1, 2 and 4 h^{-1}, were tested. The obtained hydrocracking product distributions are summarized in Table **4**.

Table 5: Effect of Reaction Temperature on Composition of OLPs as a Function of LHSVs (Pressure=6MPa, H_2/Oil Ratio = 400 v. /v.)

LHSV,h^{-1}		4				2				1			
Reaction Temperature,°C		375	400	425	450	375	400	425	450	375	425	425	450
n-alkanes yield,wt.%	≤ C_9	17.9	19.7	24.5	25.0	21.5	23.2	26.3	25.9	--	23.8	26.0	27.6
	C_{10}-C_{18}	51.2	49.5	40.4	38.0	45.5	42.3	40.2	35.2	--	39.6	33.8	29.3
	C_{15}	4.0	7.9	7.2	8.6	3.1	6.0	6.6	7.7	--	5.1	7.4	7.5
	C_{16}	11.4	11.3	8.2	7.7	10.2	11.0	11.3	7.3	--	9.8	9.4	5.9
	$C_{17}C_{18}$	6.2	3.6	2.0	2.65	5.9	3.9	4.2	3.6	--	6.8	4.3	2.0
	>C_{18}	22.6	12.6	6.0	5.6	19.2	10.7	5.4	3.0	--	13.8	5.3	1.4
	C_{18}/C_{17}	4.4	2.5	1.3	1.4	4.1	1.5	0.8	0.5	--	1.7	1.1	0.6
	C_{18}/C_{15}	3.6	3.5	3.0	2.2	3.3	2.8	1.3	0.8	--	2.0	1.2	0.7
	C_{16}	1.5	0.7	0.4	0.3	1.4	0.1	0.3	0.2	--	0.9	0.3	0.1

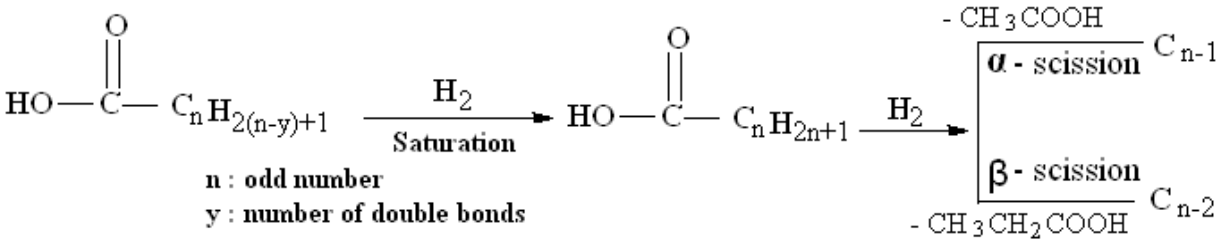

Scheme 3: α/β–C Scission pathway for conversion of fatty acids to alkanes.

From Table **4**, an overall decrease trend for the conversion is observed with increasing the LHSV; the high LHSV might suppress the cracking reactions. The ≤ C_9 yield decreases, while the yields of C_{10}-C_{18} increase, with the increase of LHSV (Table **5**). This may indicate that the residence time was not sufficient for hydrodeoxygenation and thereafter to crack the n-paraffins at higher LHSVs. Therefore, increasing the LHSV can lead to relatively higher kerosene/diesel fraction yield due to suppressed cracking (Table **4**). Furthermore, as shown in Table **5**, the C_{18}/ C_{17} and C_{18}/C_{15}-C_{16} ratios have similar behaviors, indicating that the LHSV has no significant effect on HDO and DCO/DCO_2 reactions. This fact seems to run in harmony with the results of Sankaranarayamen [29].

3.2.3. Effect of Pressure

Usually, the operating pressure has a strong effect on hydrogenation and cracking reactions of WCO. For this study, several experiments were conducted at two different pressures, namely, 2 and 6 MPa (cf., Tables **4** and **6**). The yield of kerosene/diesel in the liquid product decreases while the yield of gasoline increases, with the increase of pressure (Table **4**). It is of special interest to notice that the pressure seems to have an opposite effect on C_{17} yield. As the pressure increases, the C_{17} wt % decreases, while the C_{18} wt % increases. This difference may be mainly caused by the different routes to form C_{17} (DCO/DCO_2) and C_{18} (HDO) paraffins. Also, the variation in C_{18}/C_{17} and C_{18}/C_{15}-C_{16} ratios in the final OLP was investigated, as shown in Tables **5** and **7**. Both ratios show almost linear increases with increasing the pressure, indicating that the HDO and DCO/DCO_2 reactions, including the α/β-C scission reactions, are not just simply competitive. Considering the hydrogen consumption is a function of H_2 pressure, higher H_2 pressure should enhance the adsorbed hydrogen on the surface active sites to promote HDO reaction, while it may restrain the DCO/DCO_2 reaction, *i.e*., the high pressure is more favorable to the HDO reaction. This runs in agreement with the results obtained by Guzman *et al*. [30] and Krar *et al*. [31]. H_2 may be necessary to avoid deactivation of the catalyst by scavenging the deactivating surface species [32, 33]. Moreover, H_2 is needed to split off the fatty acids from the glycerides for further reactions [34].

3.3. OLPs Specification

The most effective way for improving the cold flow (pour point) properties of kerosene / diesel fuels is the catalytic hydrocracking [35, 36]. An inherent property of

Table 6: Effect of Reaction Temperature on Hydrocracking of WCO Feedstock (Pressure=2MPa, LHSV= 4h^{-1}, H_2/Oil Ratio=400 V/V)

Reaction Temperature, °C		375	400	425	450
Conversion, wt. %		66.0	76.0	87.0	90.0
Residual oil , wt%, 400^+ °C		34	24	13	10
Product distribution Yield, wt. %	Gaseous	6.0	7.0	9.0	11.5
	OLP	57.0	64.0	72.0	72.0
	Aqueous phase	3.0	5.0	6.0	6.5
OLP composition, wt. %	Naphtha 45/180°C	18	30	42	45
	Kerosene/diesel 180/400°C	39	34	30	27

Table 7: Effect of Reaction Temperature on Composition of OLP (Pressure=2MPa, LHSV=4h^{-1}, H_2/Oil Ratio=400 V. /V.)

n-Alkanes Yield, wt%	Reaction Temperature, °C		
	400	425	450
≤ C_9	9.6	16.6	21.8
C_{10}-C_{18}	39.7	40.0	39.0
C_{15}	6.2	6.3	5.5
C_{16}	10.6	7.1	6.8
C_{17}	6.5	8.0	11.0
C_{18}	10.2	4.5	2.2
>C_{18}	14.7	15.5	11.2
C_{18}/C_{17}	1.6	0.6	0.2
C_{15}-C_{16}/C_{18}	0.6	0.3	0.18

most hydrocracking catalysts is the formation of some amounts of lighter products, primarily naphtha (Tables **4** and **7**). The pour point, density and kinematic viscosity of the OLPs decrease with increasing the temperature and pressure, and by decreasing the LHSVs, apparently due to lightness of the fuel products (Table **8**). Generally, the results obtained show that the fuels derived from WCO possess fairly acceptable value, from their properties studied, when compared to those of the petroleum-based fuel [34]. Accordingly, the applied operating conditions in this work can be used to control the composition and properties of the projected fuel products.

3.4. Kinetic Study

Figure **2** allows us to determine the reaction order of the catalytic hydrocracking of WCO over sulfided NiW/SiO_2-Al_2O_3 catalyst, at different temperatures, namely, 375° C, 400° C, 425° C, and 450° C. The linear kinetic plots of the conversion of WCO to liquid fuels, obtained with reaction time up to 1h, under the assigned operating conditions (LHSV of 1,2,4 h^{-1}, 6.0 MPa operating pressure, and 450 v/v H_2/oil ratio), fit well with the second-order mechanism [37,38]. Moreover, the dependence of the reaction rate constants (k_2), derived from Figure **2**, on the temperature is represented by the Arrhenius equation, as:

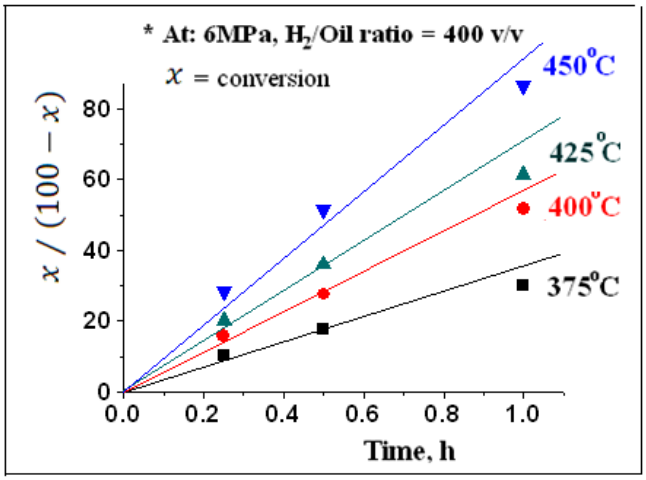

Figure 2: Plot of conversion (X) versus time of reaction for varying temperature.

$$lnk_2 = lnA - E_a/RT$$

where, A is the frequency factor, E_a is the apparent activation energy, R is the universal gas constant, and T is the absolute reaction temperature (Figure **3**). The estimated activation energy for the reaction under the mentioned conditions was 56 kJ mol^{-1}.

4. CONCLUSION

In the present study, we have examined the performance of NiW/SiO_2-Al_2O_3 catalyst in conversion

Table 8: Effect of Reaction Temperature on Physicochemical Properties of OLPs as a Function of LHSVs (Pressure=6MPa, H_2/Oil Ratio=400 V /V)

LHSV,h^{-1}	4				2				1			
Reaction Temperature,°C	375	400	425	450	375	400	425	450	375	425	425	450
Density (20°C), gm/ml	0.8465	0.8235	0.8166	0.8091	0.8382	0.8111	0.8069	0.7998	0.8290	0.8000	0.7954	0.7837
Kinematic Viscosity (40°C), mm^2/s	6.6	2.65	2.23	1.98	6.4	2.044	1.864	1.5	5.4	1.53	1.84	0.97
Pour point, °C	-12	-18	-24	-27	-18	-24	-27	-30	-24	-30	-33	-36

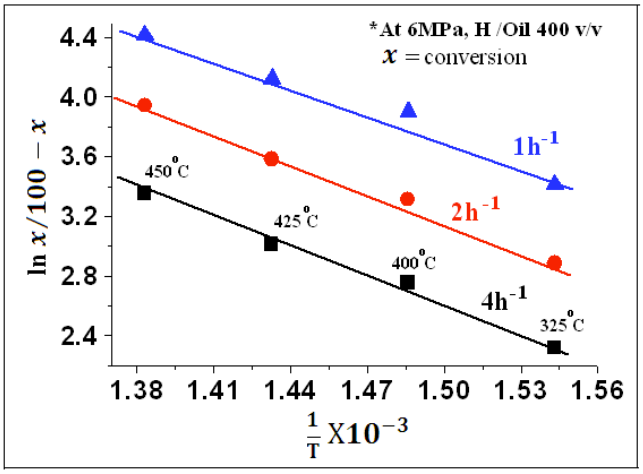

Figure 3: Arrhenius plots for hydrocracking of WCO at 6MPa, 375-450°C, for various LHSV.

of WCO to alternative fuels. Three main hydrocracking operating parameters of reaction temperature, pressure, and LHSV were studied. The results have shown that the catalytic hydrocracking of WCO generates fuel that has chemical composition similar to the petroleum-based fuel. With increasing the temperature and pressure and by decreasing the LHSV, the amount of kerosene/diesel decreased, whereas gasoline fraction increased. A considerable elimination of O_2 from vegetable oil molecules have been indicated by FTIR analysis. A kinetic study was carried out to determine the reaction order and the apparent activation energy (E_a) of the catalytic hydrocracking of WCO over the sulphided $NiW/SiO_2Al_2O_3$ catalyst, under the operating conditions: LHSV of 1,2,4 h^{-1}, 6.0 MPa operating pressure and 450 v/v H_2/oil ratio and at temperatures ranged between 375° C and 450° C. The reaction was found to follow the second order mechanism with activation energy of 56 kJ mol^{-1}.

ACKNOWLEDGEMENT

The authors are greatly indebted to Prof. Salah A. Hassan for appreciated assistance and numerous useful discussions throughout this work.

REFERENCES

[1] Choudharry TV, Phillips CB, Appl. Catal. A 2011; 397:1-12.

[2] Naik SN, Rout PK, Dalai AK. Renew Sustain Energy Rev. 2010; 14:578-597.

[3] Corma A, Iborra S, Velty A. Chem Rev 2007; 107:2411-2502.

[4] Huber G, Iborra S, Corma A. Chem Rev 2006; 106:4044-4098.

[5] Kamm B, Gruber PR. Kamm Eds Biorefineries-industerial process and products Wiley /VCH, Weinheim 2006.

[6] Centi G, Van Santen RA, Eds Catalysis for Renewables: From feedstock to energy production. Wiley / Vcit, Weinheim 2007.

[7] Santillan-Jimenez E, Croker M. J Chem Technol and Bio Technol. 2012; 87: 1041-1050

[8] Luis FI. J Mater Res 2013; 16: 792-802.

[9] Benazzi AE, Cameron C. Hydroc Proc 2006; 85: DD17-DD8.

[10] Ali MF, El Ali BM. Speight JG Handbook of Industrial Chemistey: McGraw-Hill, 2005.

[11] Krar M, Kovacs S, Kallo D, Hancsok J Bioresour Technol 2010; 101: 9287-9293.

[12] Kubicka D, Kaluza L. Appl Catal A 2010; 372: 199-208.

[13] Boda I, Onyestyak G, Solt IT, Lony F, Valyan J. Appl Catal A 2010; 374: 158-169.

[14] Bezergianni S, Dimitriadis A, Kalogiamni A, Knudsen KG. Ind Eng Chem Res 2011; 50:3874-3879.

[15] Bezergiamni S, Dimitriadis A, Sfetsas T, Kalogiamni A. Bioresour Technol 2010; 101: 7658-7660.

[16] Yang Y, Wang Q, Zhang X, Wang L, Li G. Fuel Process. Technol 2013; 116: 165-172.

[17] Senol OI, Ryymin EM, Viljava TR, Krause AOI. J Mol Catal A 2007; 268: 1-8.

[18] Hubar GW, Q,conrar P, Corma A . Appl Catal A 2007; 329: 120-129.

[19] Toba M, Abe Y, Kuramochi H, Oska M, Mochizuki T, Yoshimura Y. Catal Today 2010; 164: 533-541

[20] Tiwari R, Rama BS, Kumar R, Verma D, Kumar R, Jashi RK, *et al*. Catal Commun 2011; 12: 559-566.

[21] Sandor K, Tamas K, Artus T, Ilona H, Jeno H. Chem Eng J 2011; 176-177: 237-244.

[22] Twaiq FAA, Zabidi, NAM, Mohamed RA, Bhatia S. Ind Eng Chem Res 2003; 38:3230-3237.

[23] Yamyang L, Rogelio SB, Kazuhisa M, Tomouki M, Kinya S. Catalysts 2012; 3:171-177.

[24] Niken T, Abdul Rahman M, Subhash B. Bioresour Technol 2011; 102: 10685-10691

[25] Anders TM, El Hadi A, Claus HC, Rasmus F, Anders R. Fuel 2011; 90:3433-3440.

[26] Rasmus E, Niels M, Lars S, Per Z. PTQ Q_2 2010; 15:101-106.

[27] Huber GW, Q'Conner P, Corma A. Appl Catal A 2007; 329:120-129.

[28] Kissin TV. Cat Rev 2001; 43:85-92.

[29] Sankaranarayamen TM, Bamu M, Panduramgan A, Sivasanker S. Bioresour. Technol. 2011; 102: 10717-10727.

[30] Guzman A, Torres JE, Prada LP, Nunez ML, Catal.Today 2010; 156:38-43.

[31] Krar M, Kovacs S, Kallo D, Hancsok J. Bioresour Technol 2010; 101: 9287-9293.

[32] Maki-Arvela P, Kubickova I, Snare M, Eranem K, Murzin D. Energy Fuels 2007; 21: 30-41.

[33] Donnis B, Egeberg RG, Blom P, Knudsen KG. Top Catal 2009; 52: 229-240.

[34] Xu J, Jiang J, Chen J, Sun Y. Bioresour Technol 2010; 101: 5586 -5591.

[35] Per Z, Henrik R. Hydrocarbon Eng 2012; 17:39-47.

[36] Peter B, Rasmus G. Hydrocarbon Eng 2012; 17: 31-38.

[37] Witckakorn C, Tharapong V. Energy Fuels 2005; 19: 1783-1789.

[38] Dieter L, Energy Fuels 2008; 22 231-236

Received on 10-10-2014 Accepted on 03-10-2014 Published on March-2015

http://dx.doi.org/10.15379/2408-9834.2015.02.01.3